

# NMR $^1\text{H}$ -Shielding Constants of Hydrogen-Bond Donor Reflect Manifestation of the Pauli Principle

M. Natalia C. Zarycz<sup>\*,†,‡,§</sup> and Célia Fonseca Guerra<sup>\*,§,||</sup>

<sup>†</sup>Instituto de Investigaciones en Físico-Química de Córdoba, (INFIQC), CONICET, Facultad de Ciencias Químicas, Universidad Nacional de Córdoba, Haya de la Torre esq. Medina Allende, X5000HUA Córdoba, Argentina

<sup>‡</sup>CONICET-CCT Nordeste, Facultad de Ciencias Exactas, Naturales y Agrimensura, Universidad Nacional del Nordeste, Av. Libertad 5460, W3400AAS Corrientes, Argentina

<sup>§</sup>Department of Chemistry and Pharmaceutical Sciences and Amsterdam Center for Multiscale Modeling (ACMM), Vrije Universiteit, Amsterdam, De Boelelaan 1083, 1081 HV Amsterdam, The Netherlands

<sup>||</sup>Leiden Institute of Chemistry, Gorlaeus Laboratories, Leiden University, P.O. Box 9502, 2300 RA Leiden, The Netherlands

## Supporting Information

**ABSTRACT:** NMR spectroscopy is one of the most useful methods for detection and characterization of hydrogen bond (H-bond) interactions in biological systems. For H bonds  $\text{X}-\text{H}\cdots\text{Y}$ , where X and Y are O or N, it is generally believed that a decrease in  $^1\text{H}$ -shielding constants relates to a shortening of H-bond donor–acceptor distance. Here we investigated computationally the trend of  $^1\text{H}$ -shielding constants for hydrogen-bonded protons in a series of guanine C8-substituted GC pair model compounds as a function of the molecular structure. Furthermore, the electron density distribution around the hydrogen atom was analyzed with the Voronoi deformation density (VDD) method. Our findings demonstrate that  $^1\text{H}$ -shielding values of the hydrogen bond are determined by the depletion of charge around the hydrogen atom, which stems from the fact that electrons obey the Pauli exclusion principle.

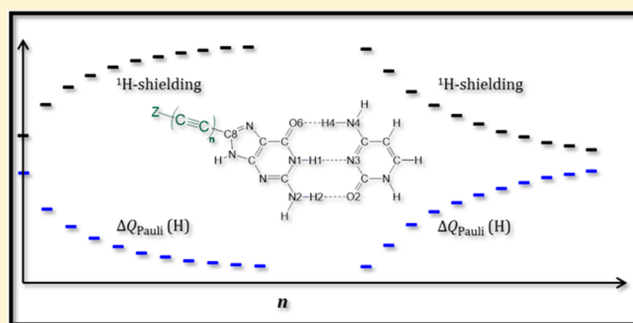
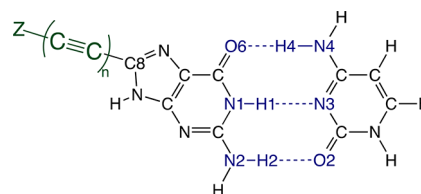


Chart 1. Nanoswitch Model Systems Based on Substituted Watson–Crick GC Pair



Hydrogen bonds (H bonds) are one of the most important interactions in a wide range of chemical processes because they play a key role in phenomena including substrate–enzyme reactions, self-assembly of nanomaterials, and molecular recognition; for example, they are essential to the working of the genetic code in DNA, in protein folding, and also in advanced drug and materials design.<sup>1–9</sup> Therefore, the understanding of factors that determine H-bond properties and, as a consequence, those of molecular systems in which they intervene, has been and is a field of intense research.<sup>10</sup> In particular, NMR spectroscopy is one of the main techniques for experimentally characterizing H-bond interactions,<sup>11,12</sup> and computational studies have been devoted to explain the observations.<sup>13–20</sup>

Previous theoretical studies have examined the effect on the H bonding of DNA base pair GC,<sup>21</sup> when anionic, neutral, or cationic substituents were introduced at the C8 position of guanine through a  $\pi$ -conjugated linker of acetylene units,  $-(\text{C}\equiv\text{C})_n-$  (see Chart 1). The computations demonstrated the possibility to build a supramolecular nanoswitch based on the DNA base pair GC that can be chemically switched in a remote way, over a distance of up to nearly 3 nm, between three states that differ in hydrogen-bond strength: weak, intermediate, and strong. These results are relevant for potential applications in supramolecular chemistry<sup>22</sup> and

antisense technology.<sup>23</sup> In these studies, it was also shown that introducing acetylene units yields a gradual variation of H-bond lengths of GC, which makes these systems very suitable for the investigation of properties of hydrogen bonds with the same basic molecular structure.

In this work, we investigate the NMR  $^1\text{H}$  nuclear magnetic shielding constant behavior of the hydrogen-bond donors (H4, H1, and H2) as a function of the molecular structure in the model systems of Chart 1, within the framework of the density functional theory (DFT).<sup>24</sup> It is known that when a hydrogen

Received: May 12, 2018

Accepted: June 21, 2018

Published: June 21, 2018

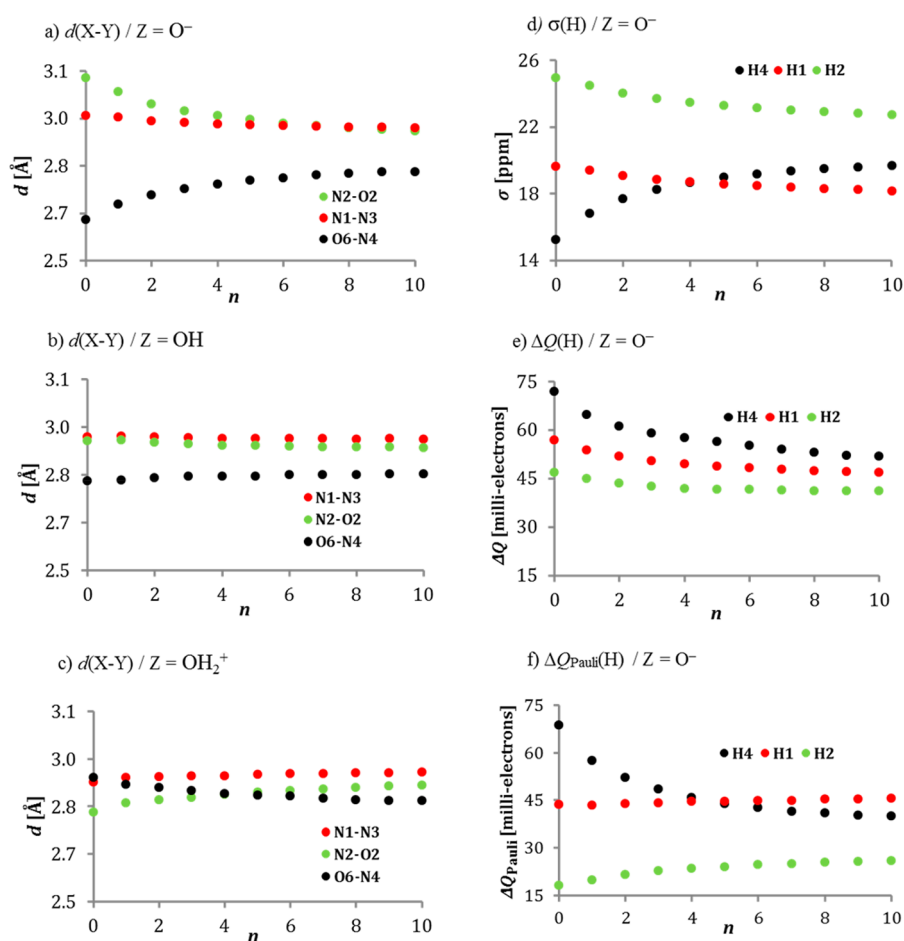


**Figure 1.** (a) H-bond lengths in  $Z-(C\equiv C)_n-GC$  with  $Z = O^-$ , (b)  $Z = OH$ , and (c)  $Z = OH_2^+$ . (d)  $^1H$ -shielding values for H4, H1, and H2 in  $O^--(C\equiv C)_n-GC$ . (e)  $\Delta Q$  of H4, H1, and H2 in  $O^--(C\equiv C)_n-GC$ . (f)  $\Delta Q_{Pauli}$  of H4, H1, and H2 in  $O^--(C\equiv C)_n-GC$  (see also Chart 1).

atom is part of a H bond,  $X-H\cdots Y$ , where X and Y are electronegative atoms, its isotropic NMR nuclear magnetic shielding constant, ( $^1H$  shielding or  $\sigma(H)$ ), undergoes a decrease; that is, the  $^1H$  NMR signal suffers a displacement to downfield. The shift of the  $^1H$  signal to higher frequencies has been associated with a shortening of the H bond; that is, the shorter the H bond, the larger the proton deshielding.<sup>4,12,25</sup> Several studies have attempted to find a correlation between H-bond lengths and  $^1H$  shieldings. Although the shape of this relationship is unclear and cannot be generalized (for some hydrogen-bond distance intervals, a linear relationship was found, but when the interval is extended, that kind of dependence is not kept), all studies suggest that when the donor–acceptor distance decreases,  $^1H$  shielding becomes smaller.<sup>4,25</sup> The downfield shift upon H-bond formation is mostly explained by the loss of electron density around the hydrogen nucleus,<sup>11,26–28</sup> although it was also suggested that the electronic currents of the acceptor atom provide deshielding effects at the proton site.<sup>29</sup> Other theoretical studies showed that  $^1H$  shielding is determined by  $\sigma$ -type orbital contribution, although in the case of the H-bonded proton, it was shown that  $^1H$ -shielding contributions due to bonds and lone pairs of the acceptor atom are negligible.<sup>26,30–32</sup> Furthermore, hydrogen bonds have a partial covalent character: The unoccupied  $\sigma_{N-H}^*$  orbital accepts electronic density from the lone pair of the opposite nitrogen or oxygen atom, which would actually lead to an accumulation

of electronic density on the hydrogen atom.<sup>33</sup> In this work, we aim to clarify the electronic contributions in hydrogen bonds that give rise to the observed trend in  $^1H$ -shielding values.

To understand the NMR  $^1H$  shielding in hydrogen bond donors, we analyzed the electron density distribution around the hydrogen atom using the Voronoi deformation density (VDD) method.<sup>34,35</sup> In the VDD method, the electronic accumulation or depletion per atom,  $\Delta Q(A)$ , is quantified upon the formation of a hydrogen-bonded complex from two monomers.

The VDD method partitions the space into so-called Voronoi cells, which are nonoverlapping regions of space that are closer to a given nucleus A than to any other nucleus. The change in VDD atomic charges of the front atoms (H4, H1, and H2),  $\Delta Q(A)$ , upon the formation of a hydrogen-bonded complex from two monomers is defined by

$$\Delta Q(A) = - \int_{\text{Voronoi cell of A in dimer}} (\rho_{\text{dimer}}(\mathbf{r}) - \rho_1(\mathbf{r}) - \rho_2(\mathbf{r})) \mathbf{d}\mathbf{r} \quad (1)$$

Equation 1 relates  $\Delta Q(A)$  directly to the deformation density,  $\rho_{\text{dimer}}(\mathbf{r}) - \rho_1(\mathbf{r}) - \rho_2(\mathbf{r})$ , associated with forming the overall molecule (i.e., the base pair) from the joining of monomers 1 and 2 in the geometry of the complex.  $\Delta Q(A)$  has a simple and transparent interpretation: It directly monitors how much charge flows out of ( $\Delta Q(A) > 0$ ) or into ( $\Delta Q(A) < 0$ ) the

Voronoi cell of atom A as a result of the chemical interactions between monomers 1 and 2 in the dimer.

The change in VDD atomic charges,  $\Delta Q(A)$ , can be further decomposed into a component associated with the rearrangement in electronic density due to Pauli repulsive orbital interactions, that is, destabilizing interactions between occupied orbitals, and that is responsible for any steric repulsion and a component associated with the bonding orbital interactions, that is, charge transfer (i.e., donor–acceptor interactions between occupied orbitals on one moiety with unoccupied orbitals of the other, including the HOMO–LUMO interactions) and polarization (empty/occupied orbital mixing on one fragment due to the presence of another fragment)

$$\Delta Q(A) = \Delta Q_{\text{Pauli}}(A) + \Delta Q_{\text{oi}}(A) \quad (2)$$

Moreover, each of these terms can also be decomposed into contributions from the  $\sigma$ - and  $\pi$ -electron systems. In previous work,<sup>36</sup> it was shown that  $\Delta Q_{\text{Pauli}}$  of the H-bonded protons in the GC pair are dominated by  $\sigma$ -orbital contributions. As our computational analyses will demonstrate,  $^1\text{H}$ -shielding values of H bonds are governed by the Pauli repulsion interaction, which originates from the fact that electrons with the same spin are not allowed to be at the same position in space, and are a manifestation of the Pauli principle. The importance of Pauli repulsion was previously shown for the relative hydrogen-bond length and strength of the GG and CC mismatched base pairs.<sup>37</sup>

All of our computations were carried out within the framework of the DFT theory. Geometry optimizations were performed in  $C_s$  symmetry at  $\omega$ -B97XD/6-311++G(d,p), and  $^1\text{H}$ -nuclear magnetic shieldings were obtained at the GIAO/B3LYP/cc-pVTZ level using the Gaussian 09 program package.<sup>38</sup> Cartesian coordinates of all model systems are provided in the Supporting Information. Voronoi deformation density analysis was done at the BLYP-D3(BJ)/TZ2P level with the Amsterdam Density Functional (ADF) program (2017.107). See the Supporting Information for additional specification of all mentioned methodologies.

Our results are collected in Figure 1. Further details are provided in the Supporting Information. The most significant variation of H-bond lengths as a function of the linker size  $n = 0$  to 10 is obtained in the case of  $Z = \text{O}^-$  (see Figure 1a). Thus the upper H bond  $\text{O6}\cdots\text{H4}-\text{N4}$  expands by 0.15 Å, the middle H bond  $\text{N1}-\text{H1}\cdots\text{N3}$  contracts by 0.04 Å, and the lower H bond  $\text{N2}-\text{H2}\cdots\text{O2}$  contracts by 0.17 Å. For  $Z = \text{OH}$  and  $Z = \text{OH}_2^+$ , changes in H-bond lengths are much smaller than for the anionic substituent as the linker is elongated, that is,  $\pm 0.02$  Å or less for the neutral substituent and  $\pm 0.09$  Å or less for the cationic group (see Figure 1b,c). Because the largest variation in bond lengths takes place for  $Z = \text{O}^-$ , we select systems with an anionic substituent as the most suitable to perform our studies on  $^1\text{H}$  shieldings and analysis of the deformation density.

For our selected systems, the  $^1\text{H}$ -shielding values for the upper H bond  $\text{O6}\cdots\text{H4}-\text{N4}$  increase by 4.40 ppm, whereas for the middle H bond  $\text{N1}-\text{H1}\cdots\text{N3}$  and the lower H bond  $\text{N2}-\text{H2}\cdots\text{O2}$  decreases by 1.46 and 2.22 ppm, respectively, as the number of  $-(\text{C}\equiv\text{C})_n-$  units increases from  $n = 0$  to 10 (see Figure 1d). Comparing trends in  $^1\text{H}$ -shieldings values with the H-bond lengths for the three H bonds as the linker is elongated from  $n = 0$  to 10, we observe the pattern that was expected from previous studies. In the case of the upper H

bond  $\text{O6}\cdots\text{H4}-\text{N4}$ , the H-bond length becomes larger with increasing linker size, and the  $^1\text{H}$  shielding moves to upfield, and in the case of H bonds  $\text{N1}-\text{H1}\cdots\text{N3}$  and  $\text{N2}-\text{H2}\cdots\text{O2}$ , the H-bond length diminishes with increasing linker size and the  $^1\text{H}$  shielding moves to downfield. Linear regression coefficient  $R^2$  for relationships between  $d(X-Y)$  versus  $\sigma(\text{H})$  are 0.997, 0.998, and 0.994 for H-bond lengths  $d(\text{O6}-\text{N4})$ ,  $d(\text{N1}-\text{N3})$ , and  $d(\text{N2}-\text{O2})$ , respectively, which confirm a very good linear correlation between both properties.

The linker  $-(\text{C}\equiv\text{C})_n-$  and the hydrogen bonds influence the electronic density around the hydrogen atoms H4, H1, and H2. These changes in electronic density can be measured with  $\Delta Q(\text{H})$  (see computational details).  $\Delta Q(\text{H})$  becomes more negative as the linker is elongated (see Figure 1e), and thus  $\Delta Q(\text{H4})$ ,  $\Delta Q(\text{H1})$ , and  $\Delta Q(\text{H2})$  become less positive by 19.96 m-e (milli-electrons), 10.11 m-e, and 5.83 m-e, respectively. Inspection of the trends followed by the  $^1\text{H}$ -shielding and  $\Delta Q(\text{H})$  values as a function of the molecular structure for the upper H bond exhibits that less loss of electronic density increases the  $^1\text{H}$  shielding (see Figure 1d,e). Comparison of the results for middle and lower H bonds shows that as the  $^1\text{H}$  shielding decreases  $\Delta Q(\text{H})$  becomes less positive. Thus the correlation between the  $^1\text{H}$  shielding and  $\Delta Q(\text{H})$  is inconsistent with our expectations based on previous studies. As previously noted, a decrease in  $^1\text{H}$  shielding is associated with a loss of the electronic density around the hydrogen atom, but for middle and lower H bonds, our results disobey this rule. So, might there be an aspect that has not been taken into account in previous theoretical formulations when the electronic charge density around the hydrogen atom is associated with the  $^1\text{H}$  shielding? To answer this question we decomposed  $\Delta Q(\text{H})$  into  $\Delta Q_{\text{Pauli}}(\text{H})$  (see Figure 1f) and  $\Delta Q_{\text{oi}}(\text{H})$  (see the Supporting Information) as the number of  $-(\text{C}\equiv\text{C})_n-$  units enlarges from  $n = 0$  to 10. In the case of the upper H bond,  $\Delta Q_{\text{Pauli}}(\text{H4})$  becomes less positive by 28.69 m-e, whereas for the middle H bond and the lower H bond,  $\Delta Q_{\text{Pauli}}(\text{H1})$  and  $\Delta Q_{\text{Pauli}}(\text{H2})$  increase by 1.88 m-e and 7.77 m-e, respectively. Comparison of the  $^1\text{H}$ -shielding and  $\Delta Q_{\text{Pauli}}(\text{H})$  values in the case of each H bond (see Figure 1d,f) shows that the trend followed by the  $^1\text{H}$  shieldings with the elongation of the linker is exactly the same as the rearrangement of the electronic density caused by the Pauli repulsion. That is, for the upper hydrogen bond, the smaller the loss of electronic density ( $\Delta Q_{\text{Pauli}}(\text{H})$  becomes less positive) as the linker elongates, the higher the  $^1\text{H}$  shielding (hydrogen atom becomes more shielded). For the middle H bond  $\text{N1}-\text{H1}\cdots\text{N3}$  and in a more pronounced way in the case of the lower H bond  $\text{N2}-\text{H2}\cdots\text{O2}$ , the larger the loss of electronic density due to Pauli repulsion ( $\Delta Q_{\text{Pauli}}(\text{H})$  becomes more positive), the lower the  $^1\text{H}$  shielding (hydrogen atom becomes more deshielded). Linear regression fits between  $\Delta Q_{\text{Pauli}}(\text{H})$  and  $^1\text{H}$  shielding give coefficients  $R^2$  of excellent quality, namely, 0.999, 0.987, and 1.000 for the upper H bond, the middle H bond, and the lower H bond, respectively. At the same time, the linear correlations between  $d(X-Y)$  and  $\Delta Q_{\text{Pauli}}(\text{H})$  is also of excellent quality, as evidenced by  $R^2$  values, that is, 0.993, 0.977, and 0.996, for the upper H bond, the middle H bond, and the lower H bond, respectively. These results allow us to interpret NMR parameters saying that  $^1\text{H}$ -shielding values are a measure of the fact that when fragments linked by hydrogen bonds become closer the Pauli repulsion becomes larger and vice versa.

In conclusion, our computational study shows for the first time evidence that  $^1\text{H}$ -shielding values of H-bond proton are determined by the depletion of electronic density around the hydrogen atom, which stems from the Pauli repulsion interaction upon H-bond formation and is quantified by the  $\Delta Q_{\text{Pauli}}(\text{H})$  term of the Voronoi deformation density method. This implies that  $\Delta Q_{\text{Pauli}}(\text{H})$  values can be used as descriptors of the lengths of H bonds, in the same way as  $^1\text{H}$  shieldings are employed. One of our challenges is to carry out similar studies in other molecular systems to confirm that this relationship is fulfilled as a general rule. We are also carrying out an exhaustive study of NMR  $J$ -couplings in our model systems for  $Z = \text{O}^-$ ,  $\text{OH}$ , and  $\text{OH}_2^+$  (O series) and also for  $Z = \text{NH}^-$ ,  $\text{NH}_2$ , and  $\text{NH}_3^+$  (N series) to find possible correlations with molecular properties herein investigated.

## ■ ASSOCIATED CONTENT

### Supporting Information

The Supporting Information is available free of charge on the ACS Publications website at DOI: 10.1021/acs.jpcclett.8b01502.

Further computational details. Numerical values and additional figures for  $^1\text{H}$  shieldings, VDD atomic charges analysis, and donor–acceptor distances. Details of linear regression procedures. Cartesian coordinates of all systems used in this work. (PDF)

## ■ AUTHOR INFORMATION

### Corresponding Authors

\*M.N.C.Z.: E-mail: [nzarycz@conicet.gov.ar](mailto:nzarycz@conicet.gov.ar).

\*C.F.G.: E-mail: [c.fonseca Guerra@vu.nl](mailto:c.fonseca Guerra@vu.nl).

### ORCID

M. Natalia C. Zarycz: 0000-0001-9838-5778

Célia Fonseca Guerra: 0000-0002-2973-5321

### Notes

The authors declare no competing financial interest.

## ■ ACKNOWLEDGMENTS

M.N.C.Z. thanks the “Consejo Nacional de Investigaciones Científicas y Técnicas (CONICET)” for financial support. C.F.G. thanks The Netherlands Organization for Scientific Research (NWO/CW) for financial support.

## ■ REFERENCES

- (1) Jeffrey, G. A.; Saenger, W. *Hydrogen Bonding in Biological Structures*; Springer-Verlag: Berlin, 1991.
- (2) Desiraju, G. R.; Steiner, T. *The Weak Hydrogen Bond*; University Press: Oxford, U.K., 1999.
- (3) Perrin, C. L.; Nielson, J. B. Strong Hydrogen Bonds in Chemistry and Biology. *Annu. Rev. Phys. Chem.* **1997**, *48* (1), 511–544.
- (4) Steiner, T. The Hydrogen Bond in the Solid State. *Angew. Chem., Int. Ed.* **2002**, *41*, 48–76.
- (5) Desiraju, G. R. Designer Crystals: Intermolecular Interactions, Networkstructures and Supramolecular Synthons. *Chem. Commun.* **1997**, *16*, 1475–1482.
- (6) Seeman, N. C. DNA in a Material World. *Nature* **2003**, *421*, 427–431.
- (7) Paraschiv, V.; Crego-Calama, M.; Fokkens, R. H.; Padberg, C. J.; Timmerman, P.; Reinhoudt, D. N. Nanostructures via Noncovalent Synthesis: 144 Hydrogen Bonds Bring Together 27 Components. *J. Org. Chem.* **2001**, *66* (25), 8297–8301.
- (8) Levinson, N. M.; Boxer, S. G. A. Conserved Water-Mediated Hydrogen Bond Network Defines Bosutinib's Kinase Selectivity. *Nat. Chem. Biol.* **2014**, *10* (2), 127–132.
- (9) Yang, C.-Y.; Phillips, J. G.; Stuckey, J. A.; Bai, L.; Sun, H.; Delproposto, J.; Brown, W. C.; Chinnaswamy, K. Buried Hydrogen Bond Interactions Contribute to the High Potency of Complement Factor D Inhibitors. *ACS Med. Chem. Lett.* **2016**, *7*, 1092–1096.
- (10) Arunan, E.; Desiraju, G. R.; Klein, R. A.; Sadlej, J.; Scheiner, S.; Alkorta, I.; Clary, D. C.; Crabtree, R. H.; Dannenberg, J. J.; Hobza, P.; Kjaergaard, H. G.; Legon, A. C.; Mennucci, B.; Nesbitt, D. J. Defining the hydrogen bond: An Account (IUPAC Technical Report). *Pure Appl. Chem.* **2011**, *83*, 1619–1636.
- (11) Becker, E. D. Hydrogen Bonding. In *Encyclopedia of Nuclear Magnetic Resonance*; Grant, D. M., Harris, R. K., Eds.; John Wiley: New York, 1996; pp 2409–2415.
- (12) Dingley, A.; Cordier, F.; Grzesiek, S. An Introduction to Hydrogen Bond Scalar Couplings. *Concepts Magn. Reson.* **2001**, *13* (2), 103–127.
- (13) Barfield, M.; Dingley, A. J.; Feigon, J.; Grzesiek, S. A DFT Study of the Interresidue Dependencies of Scalar  $J$ -Coupling and Magnetic Shielding in the Hydrogen-Bonding Regions of a DNA Triplex. *J. Am. Chem. Soc.* **2001**, *123* (17), 4014–4022.
- (14) Swart, M.; Fonseca Guerra, C.; Bickelhaupt, F. M. Hydrogen Bonds of RNA Are Stronger than Those of DNA, but NMR Monitors Only Presence of Methyl Substituent in Uracil/Thymine. *J. Am. Chem. Soc.* **2004**, *126*, 16718–16719.
- (15) Mulder, F. A. A.; Filatov, M. NMR Chemical Shift Data and Ab Initio Shielding Calculations: Emerging Tools for Protein Structure Determination. *Chem. Soc. Rev.* **2010**, *39* (2), 578–590.
- (16) Vicha, J.; Marek, R.; Straka, M. High-Frequency  $^1\text{H}$  NMR Chemical Shifts of  $\text{Sn}^{\text{II}}$  and  $\text{Pb}^{\text{II}}$  Hydrides Induced by Relativistic Effects: Quest for  $\text{Pb}^{\text{II}}$  Hydrides. *Inorg. Chem.* **2016**, *55*, 10302–10309.
- (17) Halbert, S.; Copéret, C.; Raynaud, C.; Eisenstein, O. Elucidating the Link between NMR Chemical Shifts and Electronic Structure in d0 Olefin Metathesis Catalysts. *J. Am. Chem. Soc.* **2016**, *138*, 2261–2272.
- (18) Dračinský, M. The Chemical Bond: The Perspective of NMR Spectroscopy. *Annu. Rep. NMR Spectrosc.* **2017**, *90*, 1–40.
- (19) Zarycz, N.; Aucar, G. A. Theoretical NMR Spectroscopic Analysis of the Intramolecular Proton Transfer Mechanism in Ortho-Hydroxyaryl (Un-)Substituted Schiff Bases. *J. Phys. Chem. A* **2008**, *112* (37), 8767–8774.
- (20) Castro, A. C.; Swart, M.; Guerra, C. F. The Influence of Substituents and the Environment on the NMR Shielding Constants of Supramolecular Complexes Based on A–T and A–U Base Pairs. *Phys. Chem. Chem. Phys.* **2017**, *19*, 13496–13502.
- (21) Fonseca Guerra, C.; Szekeres, Z.; Bickelhaupt, F. M. Remote Communication in a DNA-Based Nanoswitch. *Chem. - Eur. J.* **2011**, *17*, 8816–8818.
- (22) Vogtle, F. *Supramolecular Chemistry*; Wiley: Chichester, U.K., 1993.
- (23) *Antisense Research and Application*; Crooke, S. T., Ed.; Springer Verlag: Berlin, 1998.
- (24) Kohn, W.; Sham, L. J. Self-Consistent Equations Including Exchange and Correlation Effects. *Phys. Rev.* **1965**, *140* (4A), 1133–1138.
- (25) Siskos, M. L.; Tzakos, A. G.; Gerathanassis, I. P. Accurate Ab Initio Calculations of  $\text{O}-\text{H}\cdots\text{O}$  and  $\text{O}-\text{H}\cdots-\text{O}$  Proton Chemical Shifts: Towards Elucidation of the Nature of the Hydrogen Bond and Prediction of Hydrogen Bond Distances. *Org. Biomol. Chem.* **2015**, *13*, 8852–8868.
- (26) Sternberg, U.; Brunner, E. The Influence of Short-Range Geometry on the Chemical Shift of Protons in Hydrogen Bonds. *J. Magn. Reson., Ser. A* **1994**, *108*, 142–150.
- (27) Yaday, L. D. S. *Organic Spectroscopy*; Springer-Science: Dordrecht, The Netherlands, 2005.
- (28) Babinský, M.; Bouzková, K.; Pipiška, M.; Novosadová, L.; Marek, R. Interpretation of Crystal Effects on NMR Chemical Shift

Tensors: Electron and Shielding Deformation Densities. *J. Phys. Chem. A* **2013**, *117* (2), 497–503.

(29) Ditchfield, R. Theoretical Studies of Magnetic Shielding in H<sub>2</sub>O and (H<sub>2</sub>O)<sub>2</sub>. *J. Chem. Phys.* **1976**, *65*, 3123–3133.

(30) Schindler, M.; Kutzelnigg, W. Theory of Magnetic Susceptibilities and NMR Chemical Shifts in Terms of Localized Quantities. II. Application to some Simple Molecules. *J. Chem. Phys.* **1982**, *76*, 1919–1933.

(31) Bohmann, J. A.; Weinhold, F.; Farrar, T. C. Natural Chemical Shielding Analysis of Nuclear Magnetic Resonance Shielding Tensors from Gauge-Including Atomic Orbital Calculations. *J. Chem. Phys.* **1997**, *107*, 1173–1184.

(32) Sutter, K.; Aucar, G. A.; Autschbach, J. Analysis of Proton NMR in Hydrogen Bonds in Terms of Lone-Pair and Bond Orbital Contributions. *Chem. - Eur. J.* **2015**, *21* (50), 18138–18155.

(33) Fonseca Guerra, C.; Bickelhaupt, F. M.; Snijders, J. G.; Baerends, E. J. The Nature of the Hydrogen Bond in DNA Base Pairs: The Role of Charge Transfer and Resonance Assistance. *Chem. - Eur. J.* **1999**, *5*, 3581–3594.

(34) Bickelhaupt, F. M.; van Eikema Hommes, N. J. R.; Fonseca Guerra, C.; Baerends, E. J. The Carbon-Lithium Electron Pair Bond in (CH<sub>3</sub>Li)<sub>n</sub> (n = 1, 2, 4). *Organometallics* **1996**, *15*, 2923–2931.

(35) Fonseca Guerra, C.; Bickelhaupt, F. M. Orbital Interactions and Charge Redistribution in Weak Hydrogen Bonds: The Watson–Crick AT Mimic Adenine-2,4-Difluorotoluene. *J. Chem. Phys.* **2003**, *119* (8), 4262–4273.

(36) Fonseca Guerra, C.; Handgraaf, J. W.; Baerends, E. J.; Bickelhaupt, F. M. Voronoi Deformation Density (VDD) Charges: Assessment of the Mulliken, Bader, Hirshfeld, Weinhold, and VDD Methods for Charge Analysis. *J. Comput. Chem.* **2004**, *25*, 189–210.

(37) van der Lubbe, S. C. C.; Fonseca Guerra, C. Hydrogen Bond Strength of CC and GG Pairs is Determined by Steric Repulsion: Electrostatics and Charge Transfer Overruled. *Chem. - Eur. J.* **2017**, *23*, 10249–10253.

(38) Frisch, M. J.; Trucks, G. W.; Schlegel, H. B.; Scuseria, G. E.; Robb, M. A.; Cheeseman, J. R.; Scalmani, G.; Barone, V.; Mennucci, B.; Petersson, G. A.; Nakatsuji, H. *Gaussian 09*; Gaussian, Inc: Wallingford, CT, 2009.